Altered Morphology, Nuclear Stability and Adhesion of Highly Metastatic Derivatives of Osteoblast-like SAOS-2 Osteosarcoma Cells

ROMAN MUFF, NATALIE NIGG, PHILIPP GRUBER, DENISE WALTERS, WALTER BORN and BRUNO FUCHS

Laboratory for Orthopaedic Research, Department of Orthopaedics, Balgrist University Hospital, University of Zurich, Zurich, Switzerland

Abstract. *Background: Metastasis is the leading cause of death in patients with osteosarcoma (OS). High alkaline phosphatase (ALP) activity and resistance to chemotherapy are independent predictors of poor clinical outcome of osteosarcoma. Here, the osteoblastic phenotype, cell and nuclear morphology, cell adhesion and drug resistance of the SAOS-2 cell line and two in vivo selected highly metastatic derivatives, LM5 and LM7, were compared. Results: ALP activity and deposition of mineralized extracellular matrix were the same in the parental SAOS-2 and the LM5 and LM7 cells, but parathyroid hormone (PTH)-stimulated cAMP accumulation was lost in the LM7 cells. The LM5 and LM7 cells were smaller than the parental SAOS-2 cells, and 10% of the LM7 cells had distorted nuclei. The adhesion of LM5 and LM7 cells was decreased when compared to SAOS-2 cells. The cytotoxic responses of the SAOS-2, LM5 and LM7 cells to Cisplatin, Doxorubicin and Etoposide were indistinguishable. Conclusion: The increased metastatic potential of LM5 and LM7 as compared to SAOS-2 cells is not associated with a substantial change of the osteoblastic phenotype or of the cytotoxic response to current chemotherapeutic drugs. The decrease in cell size and altered cell adhesion, reflecting cytoskeletal rearrangement, together with increased nuclear instability and partial dedifferentiation, as revealed by the loss of PTH responsiveness in LM7 cells, may account for the higher metastatic potential of the LM5 and LM7 sublines as compared to the parental SAOS-2 cells.*

Osteosarcoma (OS) is the most common primary malignant bone tumour in adolescence. Despite surgical intervention and aggressive chemotherapy, approximately 40% of the patients relapse with metastasis alone (88%), or with both local recurrence and metastasis (12%) (1). The lungs (89%) and bones (8%) are the most frequent sites of metastasis. Osteoblastic OS is the predominant histological subtype of conventional OS (64%). Histology *per se* is not a reliable predictor of survival, but high serum levels of alkaline phosphatase (ALP) and a poor chemotherapeutic response are frequently associated with a poor clinical outcome (1-6).

Human SAOS-2 OS cells were originally derived from a primary tumour of an 11-year-old girl, and have a low metastatic potential in animal models (7). SAOS-2 cells have an osteoblastic phenotype, including high ALP activity and a cyclic AMP response to parathyroid hormone (PTH). A relationship between an osteoblastic OS cell phenotype and metastatic potential at the cellular level is not evident. In subcloning experiments, the cell population was found to be heterogeneous (8), and Jia *et al.* isolated the SAOS-2 sublines LM5 and LM7 with increasing metastatic potential from lung metastases after serial tail vein injections of parental SAOS-2 cells into nude mice (7). The cell lines provide an experimental model to study *in vitro* the morphological, biochemical and functional alterations of the osteoblastic OS phenotype associated with increasing metastatic potential.

In the present study, the osteoblastic, morphological and functional features, and drug resistance of the highly metastatic LM5 and LM7 cells were analyzed in comparison with the parental SAOS-2 cells. U2OS cells were used as a non-osteoblastic control.

Materials and Methods

Cell culture. Human SAOS-2 (HTB-85) and U2OS (HTB-96) cells were from the American Type Culture Collection (Rockville, MD, USA). The LM5 and LM7 cells were kindly provided by E.S. Kleinerman (M. D. Anderson Cancer Centre, Houston, TX, USA). The cells were cultured in Dulbecco's Modified Eagle's Medium (4.5 g/l glucose)/Ham F12 (1:1) (Invitrogen, Carlsbad, CA, USA) supplemented with 10% fetal calf serum (FCS) at 37˚C in an atmosphere of 95% air and 5% CO_2.

Correspondence to: Bruno Fuchs, Balgrist University Hospital, Forchstrasse 340, 8008 Zurich, Switzerland. Tel: +41 44 386 1661, Fax: +41 44 386 1669, e-mail: bfuchs@research.balgrist.ch

Key Words: Adhesion, alkaline phosphatase, cytotoxicity, metastasis, osteosarcoma.

Cell count, protein content and ALP. The cell density at apparent confluence and at growth arrest was determined by counting the cells after trypsinization with a Neubauer counting chamber (Brand, Wertheim, Germany). Protein content and alkaline phosphatase activity were measured in extracts of confluent cells grown in 24-well plates. The cells were rinsed with 0.9% NaCl and lysed with 20 mM Tris/HCl, pH 7.4, containing 0.1 mM $ZnSO_4$, 1 mM $MgSO_4$ and 0.1% Triton X-100 at 37˚C for 1 h. The ALP activity was measured in 100 mM Tris/glycine, pH 9.5, with 0.8 mM p-nitrophenyl phosphate as a substrate. The linear increase of the optical density at 405 nm over time was measured with a Biorad Benchmark microplate reader (Biorad, Munich, Germany) at 37˚C. The protein content of cell lysates was determined with the Biorad protein assay and with bovine serum albumin (BSA) as a standard. Optical density was measured at 595 nm.

Extracellular mineralized matrix deposition and cAMP accumulation. Mineralization was induced by culturing confluent cells in cell culture medium supplemented (+) with 15% FCS, 50 μg/ml ascorbic acid, 10 mM β-glycerophosphate and 10 nM dexamethasone for 14 days with medium renewal every two to three days. Cells cultured in cell culture medium with 10% FCS but without (–) supplements were used as controls. The cells were washed with 0.9% NaCl, fixed for 30 min with 10% formalin and washed again with 0.9% NaCl. The cells were then stained with 1.4% Alizarin Red S (Sigma, St. Louis, MO, USA) at pH 4.2 for 5 to 10 min. After 5 washing steps with distilled water, pictures were taken with a Canon IXUS50 camera. The dye was then extracted with 10% cetylpyridinium chloride in 10 mM sodium phosphate buffer, pH 7.0, and the optical density at 595 nm was measured with a Biorad Benchmark microplate reader.

cAMP accumulation was determined in confluent cells after incubation with 10 nM human calcitonin (CT; Novartis, Basel, Switzerland) or the PTH agonist chicken PTH-related protein (1-36) (chPTHrP; Novartis) at 37˚C for 15 min in cell culture medium without FCS, but supplemented with 0.1% BSA and 1 mM isobutylmethyl xanthine. cAMP was then extracted with ice-cold ethanol, 1 mM HCl and measured by radioimmunoassay as described (9).

Morphological parameters. A Nikon (Egg, Switzerland) Eclipse E600 microscope equipped with a 40x objective, a Nikon Y-FL fluorescence illumination with appropriate filters and a Kappa DX20 camera (Kappa opto-electronics GmbH, Gleichen, Germany) were used to visualize the cells, and the PicEd Cora software 8.4 (Jomesa Messsysteme GmbH, Munich, Germany) was employed to measure cell parameters. The cell volume was calculated from the diameter of freshly trypsinized cells with the equation for round spheres. For the measurement of the area of subconfluent cells and of their nuclei, the cells were seeded at low density on glass slides and cultured at 37˚C for 24 h. They were fixed with 4% formalin in phosphate-buffered saline (PBS) for 20 min, and permeabilized in cell culture medium without FCS but supplemented with 0.1% BSA and 0.1% saponin for 30 min. F-actin and nuclear DNA were then stained for 45 min in the same medium with 2 U/ml Alexa Fluor®647 phalloidin (Molecular Probes, Eugene, OR; USA) and 300 nM 4',6-diamidino-2-phenylindole (DAPI; Molecular Probes), respectively.

Cell adhesion. Sub-confluent cells were detached with PBS supplemented with 0.05% ethylenediamine tetraacetic acid. Fifty thousand cells in 2 ml cell culture medium were seeded in 6-well plates (10 cm^2/well) and allowed to adhere at 37˚C for 30 min. Non-adherent cells were decanted by rapid shaking and the wells washed twice with cell culture medium and once with PBS. After fixation with 10% formalin the cell nuclei were stained with 300 nM DAPI. Pictures from randomly chosen areas of 1.8 mm^2 (4 to 8 per well) were taken with a Nikon Eclipse E600 microscope equipped with a Kappa camera using a 10x objective. Cell counting was performed using ImageJ software (http://rsb.info.nih.gov/ij/).

Wound healing migration assay. The cells were seeded in 24-well plates (3 wells per experimental condition) at a density of approximately 60% confluence. At confluence a wound of 0.7 to 1 mm width and approximately 1 cm length was applied with a sterile metal pin. Cell debris was removed by washing twice with cell culture medium. A homogenous wound area free of cell debris was marked under the Nikon Diaphot microscope with a circle using the Nikon object marker objective. The widths of the wounds were measured immediately after wounding in the middle of the marked circle with a Nikon ocular with a graded 1 mm scale. After incubation at 37˚C for 8 h the cells were fixed with 10% formalin and stained with 0.05% crystal violet. The closure of the wounds was measured again in the marked area to calculate the migratory rate [(distance of initial wound – distance after migration)/2 x 8 h].

Cytotoxicity assay. The cells were trypsinized at mid-log growth phase and 3,000 cells were seeded in 96-well plates. The cells were allowed to adhere overnight and then treated with control medium alone or with medium containing the indicated concentrations of Cisplatin (Ebewe Pharma, Unterach am Attersee, Austria), Doxorubicin (Pfizer, New York, NY, USA) or Etoposide (Bristol Meyers Squibb, New York, NY, USA). The percentage of living cells was determined 72 h after the addition of the drugs with the WST-1 colorimetric assay (Roche Diagnostics AG, Rotkreuz, Switzerland). The percentage growth inhibition was calculated by (100 – treatment/control x100).

Data analysis. The results are means±SEM and differences between means were determined by the parametric *t*-test using the GraphPad Prism 4.01 software (San Diego, CA, USA).

Results

Osteoblastic characterisation. ALP activity, PTH-evoked cAMP production and the calcification of extracellular matrix was assessed to investigate the osteoblastic phenotype of the cell lines. The ALP activity in extracts of confluent SAOS-2, LM5 and LM7 cells was indistinguishably high when compared to that in non-osteoblastic human U2OS osteosarcoma cell extracts that amounted to 1.4±0.2 % (n=3) of that in SAOS-2 cells (Figure 1A).

Ten nM chPTHrP, unlike CT, stimulated cAMP formation in SAOS-2 and LM5 cells to a similar extent, but both hormones were minimally effective in LM7 cells (Figure 1B). In U2OS cells, on the other hand, the cAMP production was stimulated by CT but not by chPTHrP.

Alizarin Red S staining was not observed in untreated cells (Figure 1C). The SAOS-2, LM5 and LM7 cells, unlike the U2OS cells, stained positively after treatment. Photometric quantification of solubilized red deposits indicated comparable extracellular matrix calcification by the SAOS-2, LM5 and LM7 cells, that was not observed in untreated cells or in the treated U2OS cells (Figure 1D).

Morphological characterization. The subconfluent SAOS-2 cells appeared large and polygonal with round or ellipsoid nuclei (Figure 2A). The LM5 cells and their nuclei appeared elongated. The LM7 cells were smaller in size than the SAOS-2 cells and the nuclei were heterogeneous in shape and 10% of the nuclei were kidney-like or totally irregular. This was only rarely observed in the LM5 cells.

The freshly trypsinized subconfluent SAOS-2 cells had a diameter of 19.7±0.8 μm (n=27), while the diameter of the LM5 and LM7 cells was 13.7±0.6 μm (n=29; $p<0.001$) and 16.7±0.5 μm (n=34; $p<0.003$), respectively. The calculated cell volume was reduced by 65% and 41% in LM5 and LM7 cells, respectively, when compared to SAOS-2 cells (Figure 2B).

The size of adherent SAOS-2 cells defined by the area taken up by subconfluent cells was variable, ranging from 715 to 5655 μm^2 (2720±140 μm^2; n=84), while the LM5 and LM7 cells ranged from 696-2756 μm^2 (1510±90 μm^2; n=35) and from 568-4141 μm^2 (1700±130 μm^2; n=33), respectively (Figure 2B). Consistent with the observed reduction in cell volume the mean size of the LM5 and LM7 cells was reduced by 46% ($p<0.001$) and 38% ($p<0.001$), respectively, when compared to SAOS-2 cells. The size of the nuclei was measured in the same cells. The decrease in nuclear size of 36% and 38% in the LM5 and LM7 cells, respectively, as compared to SAOS-2 cells ($p<0.001$), was associated with the decrease in cell size.

The SAOS-2, LM5 and LM7 cells reached apparent confluence at 102,000±13,000 cells/cm^2 (n=35), 91,000±11,000 cells/cm^2 (n=20) and 53,000±6,000 cells/cm^2 (n=17), respectively (Figure 2C). The saturation densities of 241,000±29,000 cells/cm^2 (n=6) and 175,000±12,000 cells/cm^2 (n=4) for the SAOS-2 and LM5 cells, respectively, were comparable, and significantly higher than that of the LM7 cells (91,000±10,000 cells/cm^2 (n=3; $p<0.01$)). Consistent with the reduced cell density at confluence, the protein content per area of the cell monolayer was similarly reduced by 80% in the LM7 cells (23±4 μg/cm^2) as compared to the SAOS-2 (115±12 μg/cm^2) and LM5 (119±10 μg/cm^2) cells (Figure 2C).

The calculated cell area of apparent confluent cells and at growth arrest was indistinguishable in the LM5 cells and SAOS-2 cells. In the LM7 cells, however, it was increased by 46% ($p<0.03$) and 151% ($p<0.001$) at confluence and saturation density, respectively, when compared to the SAOS-2 cells. The cell area was also significantly increased in the LM7 cells when compared to LM5 cells ($p<0.007$).

Cell adhesion and migration. Adhesion of the SAOS-2 cells amounted to 61±7% of seeded cells (Figure 3A). The number of adhering LM5 and LM7 cells was 54% ($p<0.02$) and 58% ($p<0.005$) lower than that of the SAOS-2 cells. Migration measured in the wound healing assay was similar in the SAOS-2, LM5 and LM7 cells (Figure 3B).

Response to chemotherapeutical treatment. In the SAOS-2, LM5 and LM7 cells the half-maximal effective concentration (EC_{50}) of Cisplatin for cytotoxic growth inhibition ranged from 1.2 to 1.5 μg/ml (Figure 4). Similarly, the EC_{50} of Doxorubicin and Etoposide were between 0.03-0.09 μg/ml and 0.3-1.3 μg/ml with no obvious corrrelation between drug resistance and metastatic potential.

Discussion

At the cellular level, the relationship between an osteoblastic phenotype and/or the ALP activity, and the metastatic potential of OS is largely unknown.

Consistent with the non-osteoblastic phenotype, the human OS U2OS cell line expressed 100-fold lower levels of ALP than the SAOS-2 cells and formation of mineralized extracellular matrix was not observed. U2OS cells also failed to stimulate cAMP in response to PTH. But importantly, CT stimulated cAMP formation in these cells, a finding, which, to our knowledge, has not been reported before. In the rat osteoblast-like UMR106-06 OS subline, on the other hand, both PTH and CT stimulated cAMP formation (10). Thus the rat cells appear different from the U2OS cells. Differentiation studies could determine whether or not the U2OS cells belong to the osteoclast lineage. The metastatic potential of these cells remains controversial, as they were non-metastatic in one study (11), and highly metastatic in another study, where the malignant phenotype was reversed by overexpression of ALP (12).

Although the SAOS-2 cells used in this study exhibited an overall high ALP activity together with other osteoblastic features when compared to non-osteoblastic U2OS cells, they are heterogeneous at the cellular level as shown by subcloning experiments (8). Up to a 50-fold difference in ALP activity in subclones, which correlated with collagen synthesis and PTH-stimulated cAMP accumulation, indicated a great variability in the osteoblastic phenotype of parental SAOS-2 cells with an overall low metastatic potential. Interestingly, the SAOS-2 and *in vivo* selected highly metastatic LM5 and LM7 cell lines investigated here exhibited comparable cellular ALP activity and extracellular matrix deposition. The results were in line with the clinical observation that metastatic lesions resemble the primary tumour histologically, and that ALP activity is an

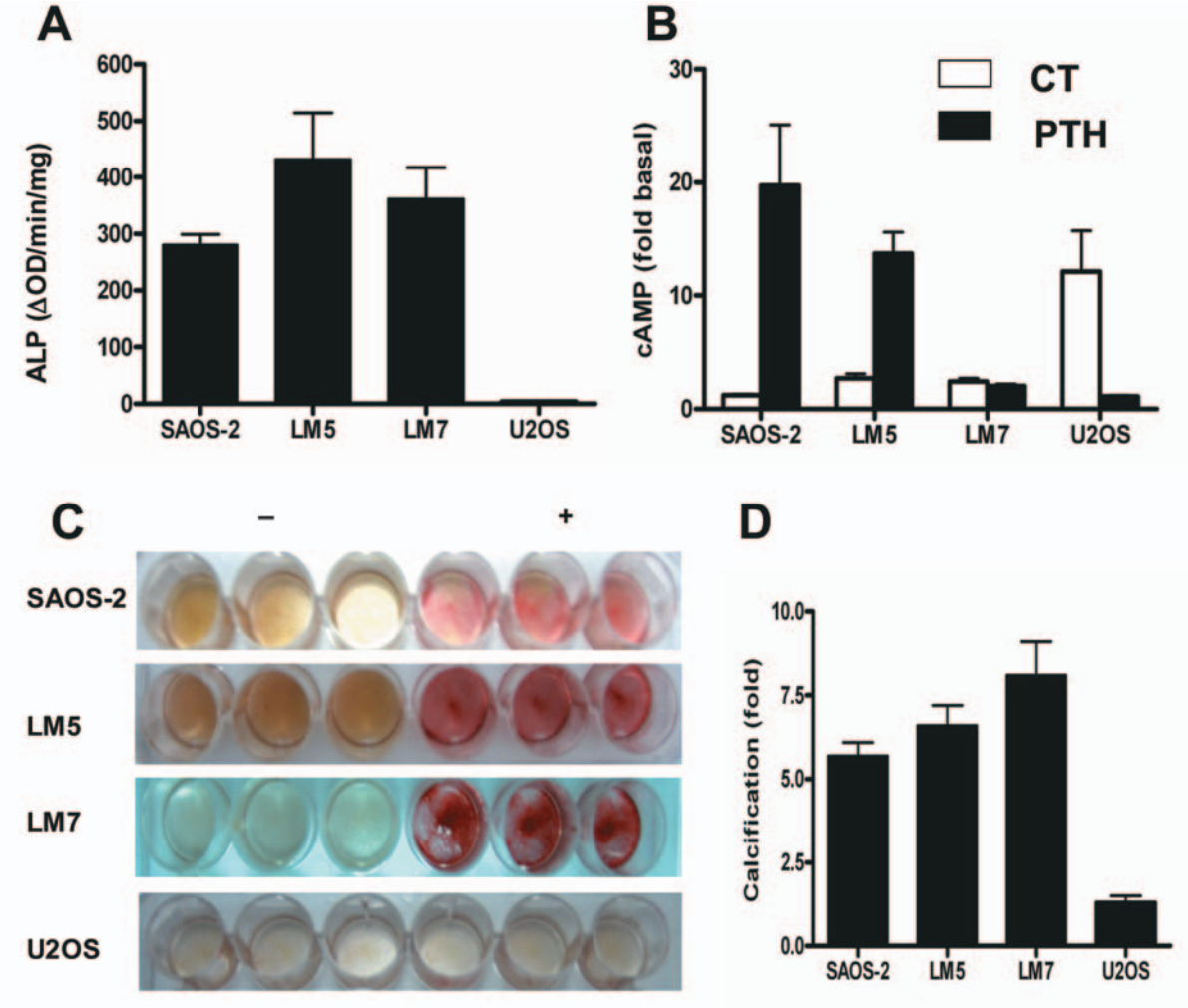

Figure 1. *Osteoblastic characterization. Alkaline phosphatase (ALP) activity in cell extracts measured at saturation density with para-nitrophenyl phosphate as a substrate (A). Cyclic AMP accumulation in confluent cells incubated at 37˚C for 15 min with 10 nM human CT (calcitonin) or chPTHrP (chicken parathyroid hormone-related protein) in the presence of 1 mM isobutylmethyl xanthine measured in cell extracts by radioimmunoassay (B). Extracellular mineral deposition, stained with Alizarin Red S, was determined in triplicates in cultures of cells maintained for 14 days in control (–) or differentiation medium (+) as described in Materials and Methods (C). Red precipitates were then solubilized with cetylpyridinium chloride and the optical density measured at 595 nm (D). Fold induction was defined as optical density of extracts from cells treated with differentiation medium divided by the optical density of extracts from non-treated cells. Results are means±SEM of at least three independent experiments carried out in duplicate.*

independent predictor of the clinical outcome (1-6). Despite their similar osteoblastic phenotype the incidence of lung metastasis increased from near zero per cent in the SAOS-2 cells to 100% in the LM5 and LM7 cells within 17 and 10 weeks, respectively, after tail vein injection (13). Thus, the LM5 and LM7 cell lines derived from lung metastatic lesions may result from *in vivo* selection of a low abundance subpopulation of highly metastatic osteoblastic SAOS-2 cells, or through the spontaneous *in vivo* acquisition or loss of poorly defined properties, which confer high metastatic potential on the SAOS-2 cells. Interestingly, the LM7 cells, unlike the SAOS-2 and LM5 cells, lost PTH responsiveness. Similarly, PTHrP overexpression in rat UMR osteoblast-like OS cells inhibited growth in an autocrine manner (14). Furthermore, a subclone of SAOS-2 cells has been shown to secrete a PTHrP-like substance (15). It remains to be shown whether escape from autocrine or paracrine growth inhibition through the loss of PTH responsiveness accounts for the earlier onset of metastasis in the LM7 as compared to the LM5 cells *in vivo*.

A higher rate of nuclear instability was observed in the LM7 as compared to the SAOS-2 and LM5 cells. Whether or not this affects the metastatic potential in osteosarcoma remains unanswered at the present time, but the occurrence of irregular nuclei correlated with poor prognosis in renal cell carcinoma (16), myeloma (17), prostate cancer (18),

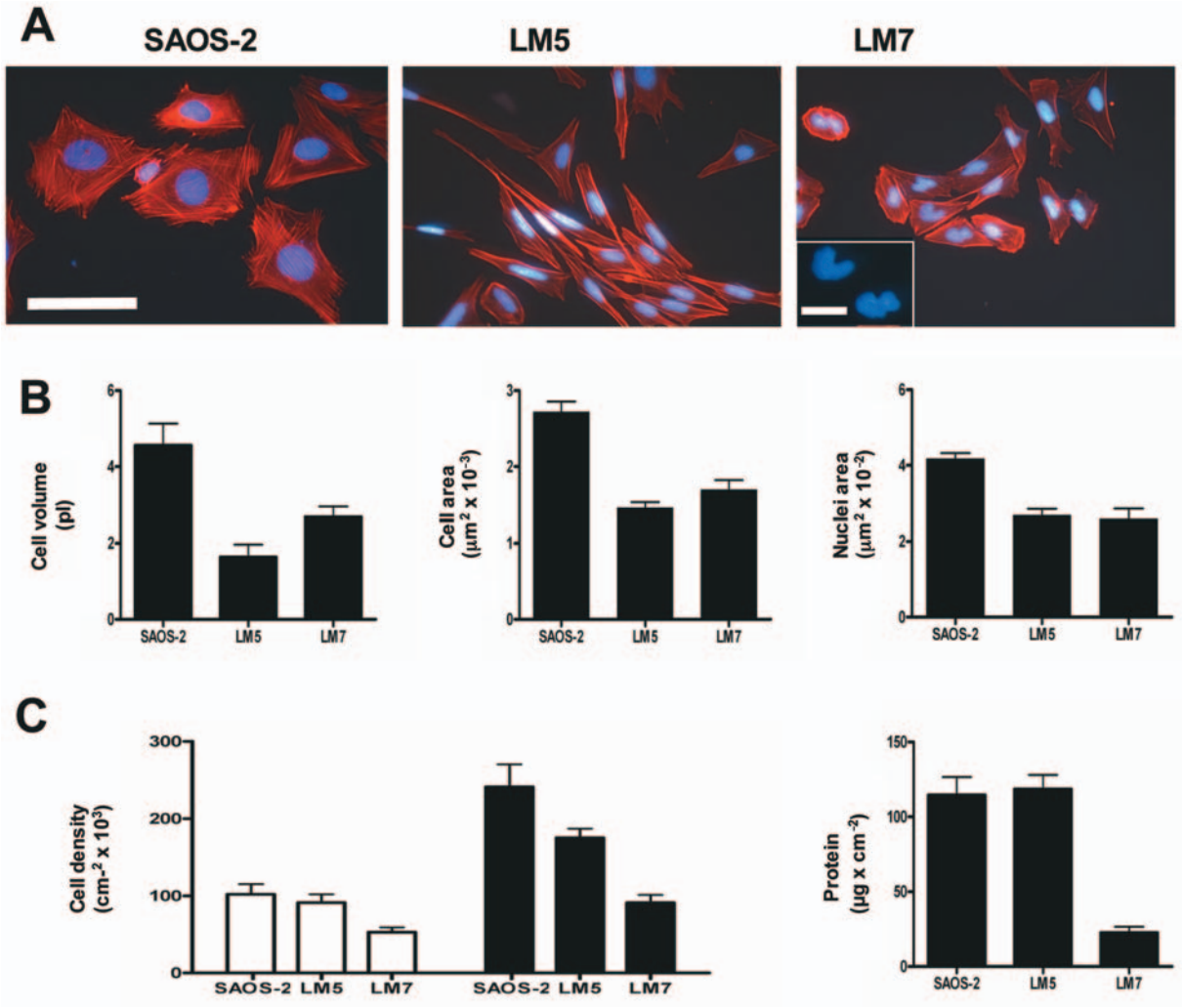

Figure 2. *Morphological characterization. Cell morphology (A). Subconfluent SAOS-2, LM5 and LM7 cells were stained for F-actin (Alexa Fluor®647 phalloidin; red) and DNA (DAPI; blue) after permeabilization with 0.1% saponin. The size bar indicates 100 µm. The insert in LM7 cells shows an irregular and a kidney-like nucleus at higher magnification, the size bar in the insert indicates 25 µm. Morphological parameters (B). Cell volume was calculated from the cell diameter measured in freshly trypsinized detached cells. Cell and nuclei areas were determined in subconfluent cells shown in Figure 1A. Cell density and protein content (C). The cell density of apparent confluent cells (white bars) and at growth arrest (black bars) was calculated by determining the cell numbers after trypsinisation. Protein content of cell extracts was measured at growth arrest. Results are means±SEM of at least 3 independent experiments.*

ovarian clear cell adenocarcinoma (19), adenocarcinoma of the lung (20), breast carcinoma (21), and leiomyosarcoma of soft tissue (22). Both the LM5 and LM7 cells were smaller in size, either attached or detached, than the parental SAOS-2 cells. This reduction in size may facilitate intravasation, retention in small vessels in the lung, extravasation and finally the formation of lung metastases. Smaller hepatocellular carcinoma cells have shown increased metastatic potential (23). A progressive decrease in adhesion from the SAOS-2 to the LM7 cells may reflect facilitated detachment from the primary tumour site and contribute to increased metastatic potential. Decreased cell adhesion to extracellular matrix in association with increased metastatic potential has been implicated, in breast cancer and colon cancer (24, 25). The similar migratory effects the LM5 and LM7 cells compared to the SAOS-2 cells was in line with the unaffected migration of LM7 cells observed in a Boyden chamber migration assay (13). Finally, the increased cell size at saturation density of the LM7 cells could explain the earlier onset of metastasis detection in LM7 (10 weeks) *versus* LM5 (17 weeks) derived metastasis, and/or the slightly increased metastatic size of the LM7 cells (13).

The growth inhibitory effects of the chemotherapeutic drugs Cisplatin, Doxorubicin and Etoposide were similar in

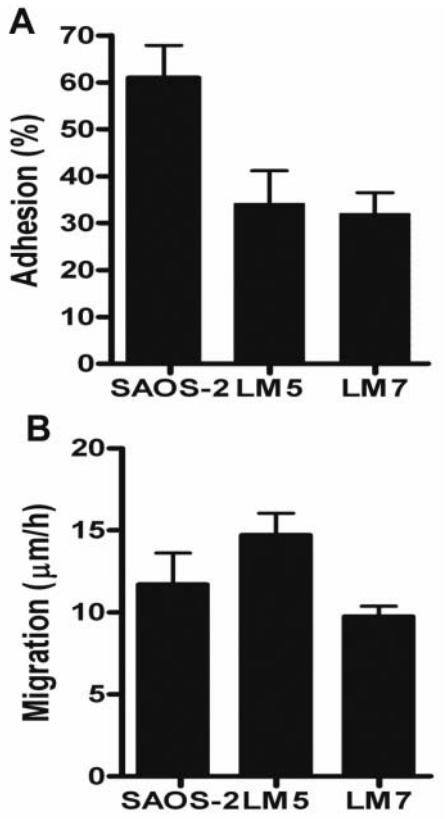

Figure 3. *Cell adhesion and migration. The number of adherent cells (A) determined by counting DAPI-stained nuclei after incubation of 50,000 cells per well for 15 min at 37˚C. Cell migration (B) was measured 8 h after wounding of confluent cells (700-1000 μm wound size) and incubation at 37˚C. The migration rate was calculated as (distance of initial wound – distance after migration)/2 x 8h. Results are means±SEM of at least 3 independent experiments.*

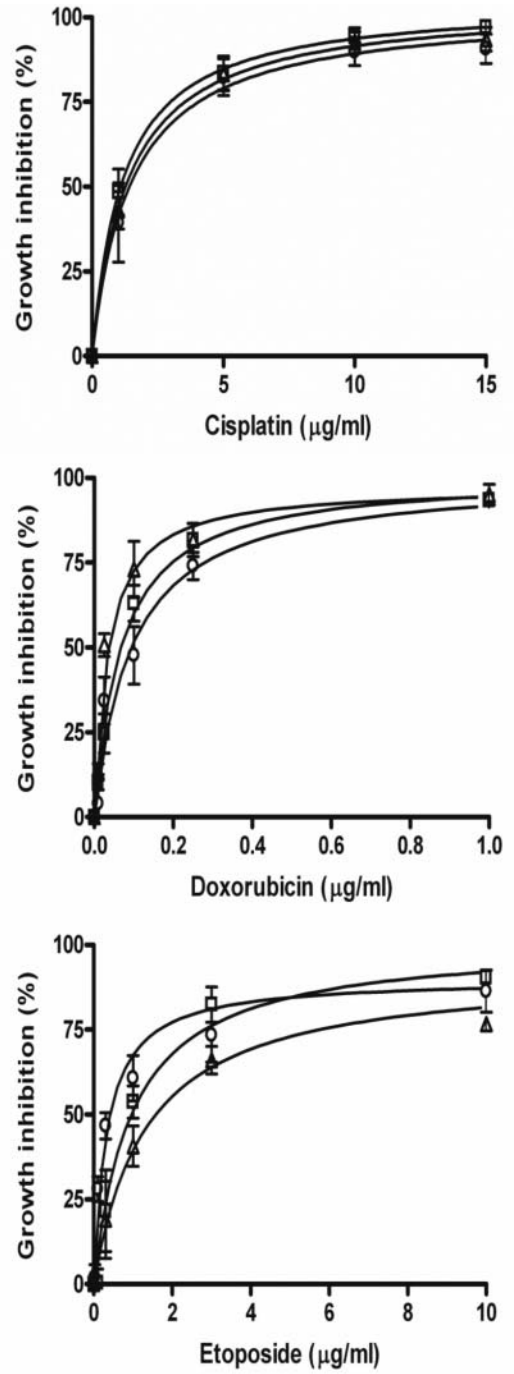

Figure 4. *Cytotoxic effect of chemotherapeutical treatment. Exponentially growing SAOS-2 (□), LM5 (△) and LM7 (○) cells were treated for 72 h with indicated concentrations of Cisplatin, Doxorubicin or Etoposide. The percentage of dead cells was determined with the colorimetric WST-1 assay. Results are means±SEM of at least three independent experiments carried out in triplicate.*

the parental SAOS-2 and in metastatically potent LM5 and LM7 cells. The results complemented those reported for Etoposide in SAOS-2 and LM6 cells (7), and indicated that drug resistance did not contribute to the increased metastatic potential of the LM5 and LM7 cells.

Taken together, the *in vivo* acquisition or loss of as yet poorly defined regulatory mechanisms affecting cell size, morphology, adhesion, migration and nuclear stability together with robust ALP expression, rather than the selection of a less differentiated phenotype, appears to contribute to the higher metastatic potential of LM5 and LM7 cells as compared to the parental SAOS-2 cells. Moreover, metastatic potential and drug resistance are not related in these cells.

Acknowledgements

This study was supported in part by Krebsliga (Zurich, Switzerland), by the WL & J Wolf Foundation (Zurich, Switzerland), by the Schweizerischer Verein Balgrist and the University of Zurich. We greatly acknowledge the receipt of LM5 and LM7 cells from ES Kleinerman, MD Anderson Cancer Center (Houston, TX, USA).

References

1 Bacci G, Longhi A, Fagioli F, Briccoli A, Versari M and Picci P: Adjuvant and neoadjuvant chemotherapy for osteosarcoma of the extremities: 27 year experience at Rizzoli Institute, Italy. Eur J Cancer *41*: 2836-2845, 2005.

2 Bacci G, Longhi A, Ferrari S, Lari S, Manfrini M, Donati D, Forni C and Versari M: Prognostic significance of serum alkaline phosphatase in osteosarcoma of the extremity treated with neoadjuvant chemotherapy: recent experience at Rizzoli Institute. Oncol Rep *9*: 171-175, 2002.

3 Mialou V, Philip T, Kalifa C, Perol D, Gentet JC, Marec-Berard P, Pacquement H, Chastagner P, Defaschelles AS and Hartmann O: Metastatic osteosarcoma at diagnosis: prognostic factors and long-term outcome-the French pediatric experience. Cancer *104*: 1100-1109, 2005.

4 Manoso MW, Healey JH, Boland PJ, Athanasian EA, Maki RG, Huvos AG and Morris CD: *De novo* osteogenic sarcoma in patients older than forty: benefit of multimodality therapy. Clin Orthop Relat Res *438*: 110-115, 2005.

5 Bramer JA, Abudu AA, Tillman RM, Carter SR, Sumathi VP and Grimer RJ: Pre- and post-chemotherapy alkaline phosphatase levels as prognostic indicators in adults with localised osteosarcoma. Eur J Cancer *41*: 2846-2852, 2005.

6 Bacci G, Longhi A, Versari M, Mercuri M, Briccoli A and Picci P: Prognostic factors for osteosarcoma of the extremity treated with neoadjuvant chemotherapy: 15-year experience in 789 patients treated at a single institution. Cancer *106*: 1154-1161, 2006.

7 Jia S-F, Worth LL and Kleinerman ES: A nude mouse model of human osteosarcoma lung metastases for evaluating new therapeutic strategies. Clin Exp Metastasis *17*: 501-506, 1999.

8 Farley JR, Hall SL, Herring S, Tarbaux NM, Matsuyama T and Wergedal JE: Skeletal alkaline phosphatase specific activity is an index of the osteoblastic phenotype in subpopulations of the human osteosarcoma cell line SaOS-2. Metabolism *40*: 664-671, 1991.

9 Moran J, Hunziker W and Fischer JA: Calcitonin and calcium ionophores: cyclic AMP responses in cells of a human lymphoid line. Proc Natl Acad Sci USA *75*: 3984-3988, 1978.

10 Forrest SM, Ng KW, Findlay DM, Michelangeli VP, Livesey SA, Partridge NC, Zajac JD and Martin TJ: Characterization of an osteoblast-like clonal cell line which responds to both parathyroid hormone and calcitonin. Calcif Tissue Int *37*: 51-56, 1985.

11 Kimura K, Nakano T, Park Y-B, Tani M, Tsuda H, Beppu Y, Moriya H and Yokota J: Establishment of human osteosarcoma cell lines with high metastatic potential to lungs and their utilities for therapeutic studies on metastatic osteosarcoma. Clin Exp Metastasis *19*: 477, 2002.

12 Manara MC, Baldini N, Serra M, Lollini PL, De Giovanni C, Vaccari M, Argnani A, Benini S, Maurici D, Picci P and Scotlandi K: Reversal of malignant phenotype in human osteosarcoma cells transduced with the alkaline phosphatase gene. Bone *26*: 215-220, 2000.

13 Duan X, Jia SF, Zhou Z, Langley RR, Bolontrade MF and Kleinerman ES: Association of avβ3 integrin expression with the metastatic potential and migratory and chemotactic ability of human osteosarcoma cells. Clin Exp Metastasis *21*: 747-753, 2004.

14 Pasquini GM, Davey RA, Ho PW, Michelangeli VP, Grill V, Kaczmarczyk SJ and Zajac JD: Local secretion of parathyroid hormone-related protein by an osteoblastic osteosarcoma (UMR 106-01) cell line results in growth inhibition. Bone *31*: 598-605, 2002.

15 Rodan SB, Wesolowski G, Ianacone J, Thiede MA and Rodan GA: Production of parathyroid hormone-like peptide in a human osteosarcoma cell line: stimulation by phorbol esters and epidermal growth factor. J Endocrinol *122*: 219-227, 1989.

16 Lohse CM, Blute ML, Zincke H, Weaver AL and Cheville JC: Comparison of standardized and nonstandardized nuclear grade of renal cell carcinoma to predict outcome among 2,042 patients. Am J Clin Pathol *118*: 877-886, 2002.

17 Leleu X, Genevieve F, Guieze R, Duhamel A, Andrieux J, Berthon C, Godon A, Prat-Lesaffre S, Depil S, Lai JL, Facon T and Zandecki M: Irregular nuclear shape of bone marrow plasma cells defines a multiple myeloma subgroup related to hypodiploidy and to short survival. Leuk Res *29*: 665-671, 2005.

18 Fischer AH, Bardarov S Jr and Jiang Z: Molecular aspects of diagnostic nucleolar and nuclear envelope changes in prostate cancer. J Cell Biochem *91*: 170-184, 2004.

19 Liu CQ, Sasaki H, Fahey MT, Sakamoto A, Sato S and Tanaka T: Prognostic value of nuclear morphometry in patients with TNM stage T1 ovarian clear cell adenocarcinoma. Br J Cancer *79*: 1736-1741, 1999.

20 Kobayashi Y, Yokose T, Kawamura K, Iwasaki S, Murata Y, Onuma S, Hasebe T, Nagai K, Sasaki S and Ochiai A: Cytologic factors associated with prognosis in patients with peripheral adenocarcinoma of the lung measuring 3 cm or less in greatest dimension. Cancer *105*: 44-51, 2005.

21 Fan F, Namiq AL, Tawfik OW and Thomas PA: Proposed prognostic score for breast carcinoma on fine needle aspiration based on nuclear grade, cellular dyscohesion and bare atypical nuclei. Diagn Cytopathol *34*: 542-546, 2006.

22 Domanski HA, Akerman M, Rissler P and Gustafson P: Fine-needle aspiration of soft tissue leiomyosarcoma: an analysis of the most common cytologic findings and the value of ancillary techniques. Diagn Cytopathol *34*: 597-604, 2006.

23 Li Y, Tang ZY, Ye SL, Liu YK, Chen J, Xue Q, Chen J, Gao DM and Bao WH: Establishment of cell clones with different metastatic potential from the metastatic hepatocellular carcinoma cell line MHCC97. World J Gastroenterol *7*: 630-636, 2001.

24 Martin TA, Watkins G and Jiang WG: KiSS-1 expression in human breast cancer. Clin Exp Metastasis *22*: 503-511, 2005.

25 Murata K, Miyoshi E, Ihara S, Noura S, Kameyama M, Ishikawa O, Doki Y, Yamada T, Ohigashi H, Sasaki Y, Higashiyama M, Tarui T, Takada Y, Kannagi R, Taniguchi N and Imaoka S: Attachment of human colon cancer cells to vascular endothelium is enhanced by N-acetylglucosaminyltransferase V. Oncology *66*: 492-501, 2004.

Received June 28, 2007
Revised October 3, 2007
Accepted October 25, 2007